Experimental retrodiction of trajectories of single photons in double interferometers

Yuan Yuan,[1,2] Zhibo Hou,[1,2] Kang-Da Wu,[1,2] Guo-Yong Xiang,[1,2,*] Chuan-Feng Li,[1,2] and Guang-Can Guo[1,2]

[1]*CAS Key Laboratory of Quantum Information, University of Science and Technology of China, Hefei 230026, China*

[2]*Synergetic Innovation Center of Quantum Information and Quantum Physics, University of Science and Technology of China, Hefei, Anhui 230026, China*

(Received 9 March 2018; published 15 June 2018)

When a photon passes through an interferometer, quantum mechanics does not provide a clear answer as to its past. Quantum retrodiction is a quantitative theory, which endeavors to make statements about the past of a system based on present knowledge. Quantum retrodiction may be used to analyze the past of a photon, that is, its trajectory. Here we experimentally retrodict the trajectories of single photons in double interferometers by measuring the final state of the photon. A sequence of measurements is made on a photon to determine which path the photon followed, so a series of retrodiction of measurement results can be regarded as a photon trajectory. We obtain information about the partial trajectory and the entire trajectory of the photon. Furthermore, we also observe the effect of different measurements in the extraction of trajectory information. Our experiment highlights the application of retrodiction theory to the study of the photon's past, and provides potential application in quantum communications.

DOI: 10.1103/PhysRevA.97.062115

I. INTRODUCTION

Prediction is concerned with future events, whereas retrodiction is concerned with past events, that is, making statements about a system's past based on the present knowledge [1]. The concepts of prediction and retrodiction are particularly relevant to basic processes involved in quantum communications [2]. With the rapid development and interest in quantum communications and quantum cryptography, quantum retrodiction theory is being studied increasingly [2–11]. Quantum retrodiction, as a quantitative theory, is applied to analyze the transmission of signals through an attenuating or amplifying channel in a quantum optical communications network [2,3] and to interpret some experimental phenomena in quantum optics, such as beam splitters [1], photon antibunching [5], and quantum scissors [7], as well as to analyze closed and open system [8,9]. It is also employed in image reconstruction from sparse photocount data [12,13], which not only focuses on a reconstructed image but also provides the full probability distribution function for the intensity at each pixel. Recently, researchers used a weak probe to continuously monitor a superconducting qubit in a microwave cavity, and with that data before and after t to retrodict the outcome of weak and strong qubit measurement performed at time t [14].

Here we are interested in retrodiction of the past of a photon in double interferometers. Quantum mechanics does not provide a clear answer to the past of a photon when it passes through an interferometer. Previous theoretical work and which-way experiments presented the past of a photon as a trajectory [15–19]. Subsequently, the study of analyzing the past of a quantum particle according to the weak trace it leaves based on the two-state vector formalism of quantum theory was proposed [20–23]. Especially, two experiments obtained anomalous trajectories of photons not always following continuous trajectories [21,22]. The experiments were performed using an asymmetric Mach-Zehnder interferometer (MZI) with a symmetric MZI inserted into one arm, and used weak interactions to mark the path that photons take through the interferometer, where the experimental results are explained in the framework of the two-state vector formalism of quantum theory [24–26]. Afterwards the analysis of the experiment in [21] using standard quantum optical methods and an amendment version were proposed [27,28]. Here we focus on the past of the photon in the double interferometers based on the quantum retrodiction method, and obtain trajectory information by measuring the final state of the photon.

Suppose a quantum system is prepared in an initial state $|\Phi\rangle$ and then subjected to a series of measurements $\{M_1, M_2, \ldots, M_N\}$, but do not read the results [see Fig. 1(a)]. Once a measurement is performed on a quantum system, the state of the system can be changed. Different measurement results correspond to different final states $|\Psi\rangle$ of the system. We can retrodict the information about measurement results just from the final state of the system. A series of measurement results can be regarded as a trajectory of the quantum system. In this paper, we experimentally retrodict the trajectories of single photons in double interferometers. A sequence of measurements is made on a photon to determine which path the photon followed, so a series of retrodiction of measurement results can be regarded as the trajectory of the photon. We are concerned with that part of or all of the measurement results, i.e., a segment of or the entirety of the photon's trajectory. Furthermore, we also observe the effect different measurements have on the extraction of the trajectory information.

*gyxiang@ustc.edu.cn

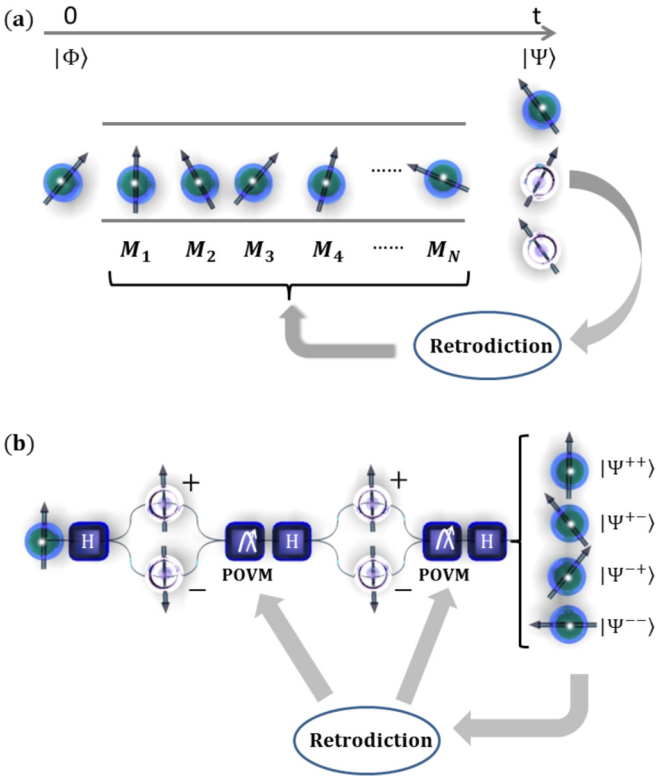

FIG. 1. (a) Concept of retrodiction from measurement results. A quantum system is prepared in an initial state $|\Phi\rangle$ at time $t = 0$ and then subjected to a series of measurements $\{M_1, M_2, \ldots, M_N\}$. Different measurement results correspond to different final states $|\Psi\rangle$ of the system. We can retrodict the information of measurement results just from the final state of the system. (b) Sketch of our experimental setup. A qubit passes a Hadamard gate (H); a positive-operator-valued measure (POVM) is then performed to obtain information about which path ($+$ or $-$) the qubit has passed through. We denote the outcomes of the measurement by $\{+,-\}$. Next, the qubit passes through a second Hadamard gate, and we perform a second POVM. Finally, it passes through the last Hadamard gate. In regard to the pair of two-outcome measurements, the output state of the qubit is in four possible states $|\Psi_{\text{out}}^{++}\rangle, |\Psi_{\text{out}}^{+-}\rangle, |\Psi_{\text{out}}^{-+}\rangle, |\Psi_{\text{out}}^{--}\rangle$. We measure the final state of the qubit to retrodict the trajectory of the qubit.

II. THEORY

Consider a qubit going through an interferometer; one generally obtains information about which path the qubit takes through that interferometer by introducing a detector (auxiliary system) in each path that discriminates detector states [29–33]. Detector states can be expressed as $|\eta(\theta)\rangle = \cos\theta|0\rangle + \sin\theta|1\rangle$ and $|\eta(-\theta)\rangle = \cos\theta|0\rangle - \sin\theta|1\rangle$ with θ ranging from 0 to $\pi/4$. The parameter θ controls how much path information is extracted from measurements. With $\theta = 0$, no path information is extracted, whereas with $\theta = \pi/4$ maximum path information is extracted. Detector states are identified through an optimal minimum error measurement $|\pm\rangle\langle\pm|$ with $|\pm\rangle = (|0\rangle \pm |1\rangle)/\sqrt{2}$. If the measurement result is $-$, the detector state is found to be $|\eta(-\theta)\rangle$, corresponding to a qubit passing through path $-$; otherwise, the qubit has passed through path $+$. If a measurement of the extraction path information is performed only on the qubit instead of the detector, then the operator corresponding to the above process is expressed as Eq. (1) [10]. The corresponding positive-operator-valued measure (POVM) operators are $\Pi_+ = A_+^\dagger A_+$ and $\Pi_- = A_-^\dagger A_-$:

$$A_+ = \frac{1}{\sqrt{2}}\begin{pmatrix}\cos\theta - \sin\theta & 0\\ 0 & \cos\theta + \sin\theta\end{pmatrix},$$
$$A_- = \frac{1}{\sqrt{2}}\begin{pmatrix}\cos\theta + \sin\theta & 0\\ 0 & \cos\theta - \sin\theta\end{pmatrix}. \quad (1)$$

The POVM is performed on the qubit, and the path information is described by the measurement results, so the detector (auxiliary system) is no longer introduced in our case. Here, we analyze a model of a qubit going through a double interferometer [10]. As illustrated in Fig. 1(b), a qubit is in the initial state $|0\rangle$ and then passes through a Hadamard gate (H), which changes the qubit in state $|0\rangle$ to state $|+\rangle = H|0\rangle$ and changes state $|1\rangle$ to state $|-\rangle = H|1\rangle$. Then we measure which path the qubit passed through (i.e., whether the qubit is in state $|0\rangle$ or $|1\rangle$) with the POVM operators. Subsequently, the qubit passes through a second Hadamard gate, and we again measure the which-path information of the qubit with POVM operators. Finally, the qubit passes through the last Hadamard gate. There are two possible measurement results for the POVM, which we denote by $+$ and $-$. Different measurement results correspond to different final states of the qubit. If both measurements yield $+$, the final state of the qubit is proportional to $|\Psi_{\text{out}}^{++}\rangle \propto HA_+HA_+H|0\rangle$; if the first measurement result is $+$ and the second measurement result is $-$, the final state of the qubit is proportional to $|\Psi_{\text{out}}^{\pm}\rangle \propto HA_-HA_+H|0\rangle$; similarly, the other two possible final states of the qubit are represented as $|\Psi_{\text{out}}^{\mp}\rangle \propto HA_+HA_-H|0\rangle$ and $|\Psi_{\text{out}}^{--}\rangle \propto HA_-HA_-H|0\rangle$. The joint probabilities for the two measurements are expressed as $P(+,+) = P(-,+) = [1 - \sin(2\theta)\cos(2\theta)]/4$ and $P(+,-) = P(-,-) = [1 + \sin(2\theta)\cos(2\theta)]/4$. The measurement results can be viewed as the "qubit trajectory" through the double interferometers. We experimentally determine what information we can obtain about the trajectory of the qubit by measuring the final state of the qubit.

III. SCHEME OF THE EXPERIMENT

We realize the above model with a linear optics system, where the qubit is encoded as $\{|0\rangle \equiv |H\rangle, |1\rangle \equiv |V\rangle\}$, and $|H\rangle(|V\rangle)$ denotes the horizontal (vertical) polarized state of the single photon. The experimental setup, illustrated in Fig. 2, consists of three modules, including the single-photon source module (see Appendix A for details), the POVM module, and the state discrimination module. The blue half-wave plates (HWPs) with an angle of 22.5° realize Hadamard gate operation. The photon starts with initial state $|0\rangle$ and then passes through HWP1, generating state $(|0\rangle + |1\rangle)/\sqrt{2}$. In the POVM modules, we use a series of birefringent calcite beam displacers (BDs) and HWPs to design POVM [34–37]. The BD causes the vertical polarized photons to be transmitted directly and the horizontal polarized photons to undergo a 4-mm lateral displacement, and hence it can split and combine the photons depending on their polarizations. So the POVM operators are realized by the setup of the BD interferometric network, which is formed by the BDs and HWPs with certain angular settings.

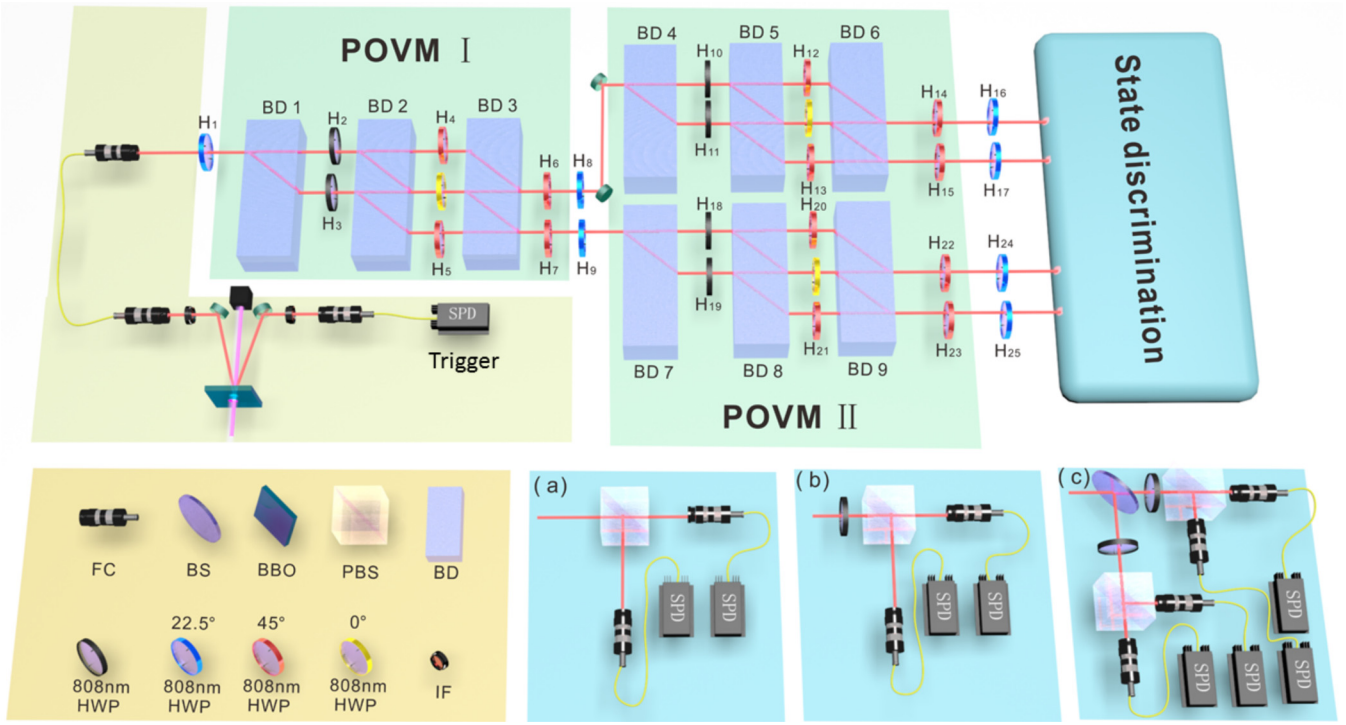

FIG. 2. Experimental setup. In the single-photon source module, the single-photon source is generated by spontaneous parametric down-conversion in a type-II beta-barium-borate (BBO) crystal used under beamlike phase-matching conditions. The blue half-wave plates (HWPs) with an angle of 22.5° perform the Hadamard gate operation. In the POVM modules, the red HWPs with an angle of 45° and beam displacers (BDs) comprise the interferometric network to perform the POVM operations; the yellow HWPs with an angle of 0° are inserted into the middle path to compensate the optical path difference between the up path and the down path; the POVM operation is changed by rotating the black HWPs. The state discrimination module is used to retrodict the POVM results. The state discrimination setups for determining the first POVM result, the second POVM result, and both are shown in Figs. 2(a)– 2(c), respectively.

The optical elements and the angle of the HWPs in the POVM I module are the same as those of the POVM II module, as they are implementing the same operator. Different POVM results correspond to the different final states of the photon. In the state discrimination module, we retrodict the partial or entire results of the POVMs made on the photon by discriminating the final states of the photon. The state discrimination setups for determining the first POVM result, the second POVM result, and both are shown in Figs. 2(a)–2(c), respectively.

IV. RESULTS OF INDIVIDUAL MEASUREMENTS

First, we would like to determine the second measurement result. The density matrix corresponding to the second measurement result $+$ is denoted as ρ_{2+}, which appears with a probability $P(\rho_{2+}) = P(+,+) + P(-,+)$. Similarly, the density matrix corresponding to the second measurement result $-$ is denoted as ρ_{2-} and appears with probability $P(\rho_{2-}) = P(+,-) + P(-,-)$. The problem of determining the second measurement result reduces to discriminating ρ_{2+} and ρ_{2-} (see Appendix B for the specific form). We use the optimal minimum-error state discrimination method to discriminate them, and find the optimal POVM elements are $\Pi_{2+} = |-\rangle\langle -|$ and $\Pi_{2-} = |+\rangle\langle +|$ [38,39]. The measurement setup for realizing the POVM elements is shown in Fig. 2(b), and the rotation angle of HWP is 22.5°. The probability of success for state discrimination is given by

$$P_s = \tfrac{1}{2}[1 + \sin(2\theta)]. \tag{2}$$

Different values of θ correspond to different POVM operators, which are realized by rotating HWP2(3), HWP10(11), and HWP18(19) in Fig. 2. The probability of success for state discrimination is plotted in Fig. 3(a). For $\theta = 0°$, the output states are identical, so the probability of success is $1/2$ by simple guess. For $\theta = 45°$, ρ_{2+} and ρ_{2-} are orthogonal and equally probable, and therefore can be discriminated perfectly. Therefore, we obtain trajectory information of the photon with certainty. Using Bayes's theorem, we define $P(\rho_{2j}|M_{\text{out}} = k)$ as the probability of ρ_{2j} occurring if the result of the measurement on the output state is $M_{\text{out}} = k$, where $j,k = \pm$. With $P(\rho_{2j}|M_{\text{out}} = k)P(M_{\text{out}} = k) = P(M_{\text{out}} = k|\rho_{2j})P(\rho_{2j})$, we find the probabilities of the occurrence of ρ_{2+} and ρ_{2-} conditioned on the measurement result of the output state. Taking the result of $M_{\text{out}} = +$ as an example, before the measurement, the probability of the state ρ_{2+} was $P(\rho_{2+})$, whereas after the measurement it was $P(\rho_{2+}|M_{\text{out}} = +)$. Figure 3(b) presents a comparison of $P(\rho_{2+})$ and $P(\rho_{2+}|M_{\text{out}} = +)$ showing that $P(\rho_{2+}|M_{\text{out}} = +) \geqslant P(\rho_{2+})$, which indicates the measurement extracts more information about the trajectory of the photon. Specifically, in Fig. 3(b) some blue circles are not on the theoretical curve because these measurement results are sensitive to change of the phase caused by the rotation of the six

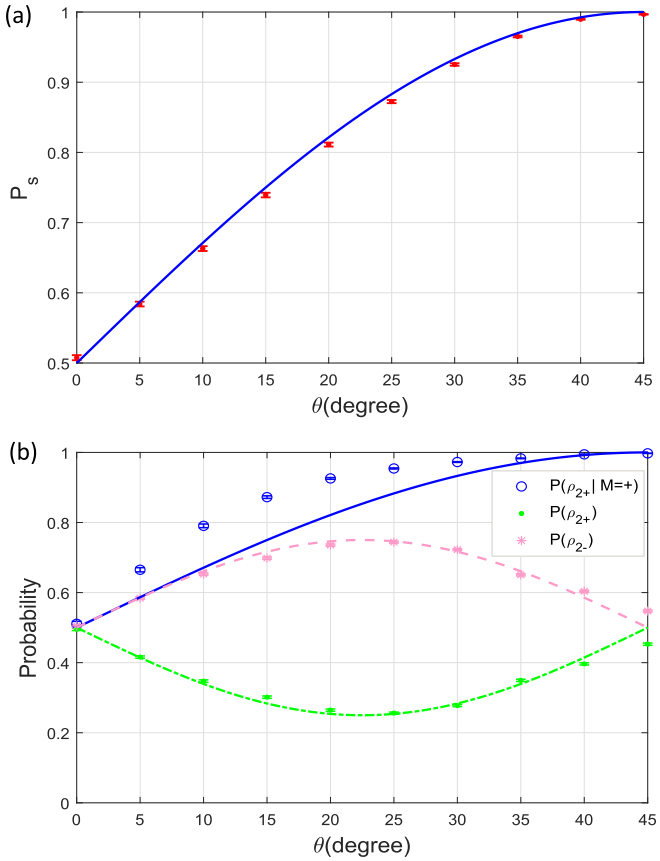

FIG. 3. (a) Experimental results for the relationship between different POVMs and retrodiction of the second measurement results; the blue line is the theoretical expectation, and the red dots are values from experimental data. (b) Comparison of $P(\rho_{2+})$ and $P(\rho_{2+}|M_{\text{out}}=+)$. The blue line and blue circles represent $P(\rho_{2+}|M_{\text{out}}=+)$ obtained using Bayes's theorem. The dash-dotted green line and green dots represent $P(\rho_{2+})$; the dashed pink line and pink stars represent $P(\rho_{2-})$.

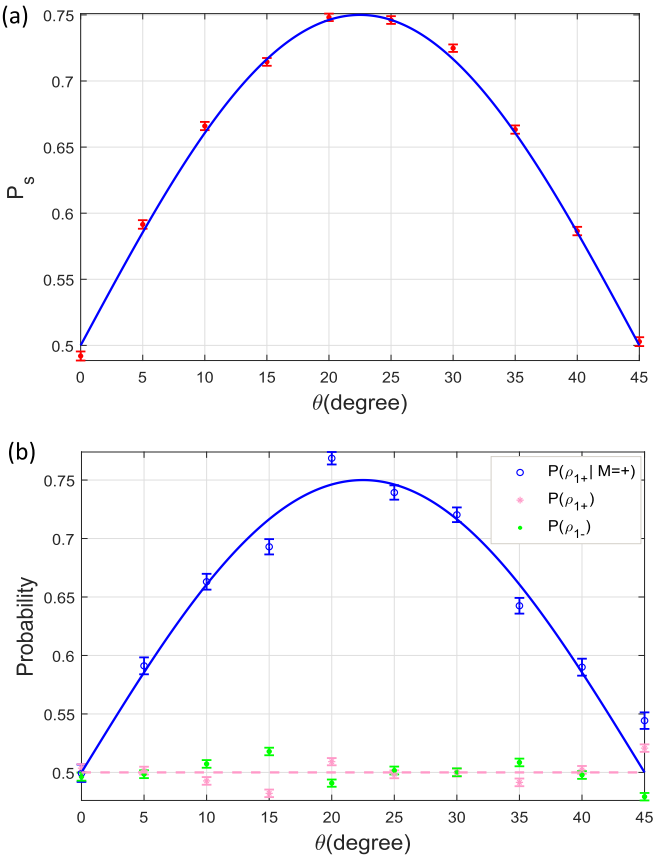

FIG. 4. (a) Experimental results for the relationship between different POVMs and retrodiction of the first measurement results. The blue line is the theoretical expectation; the red dots are values from experimental data. (b) A comparison of $P(\rho_{1+})$ and $P(\rho_{1+}|M_{\text{out}}=+)$. The blue line and blue circles represent $P(\rho_{1+}|M_{\text{out}}=+)$ obtained using Bayes's theorem. The dashed pink line is the theoretical expectation of $P(\rho_{1+})$ and $P(\rho_{1-})$. The pink stars and green dots are the experimental values of $P(\rho_{1+})$ and $P(\rho_{1-})$, respectively.

HWPs (2, 3, 10, 11, 18, and 19) inside the BD interferometric network.

Next, we determine the first measurement result. The density matrices corresponding to the first measurement results + and − are denoted as ρ_{1+} and ρ_{1-}. They appear with probability $P(\rho_{1+}) = P(\rho_{1-}) = 1/2$. The optimal POVM elements for discriminating ρ_{1+} and ρ_{1-} are $\Pi_{1+} = |1\rangle\langle 1|$, $\Pi_{1-} = |0\rangle\langle 0|$. A polarizing beam splitter (PBS) is used to realize the POVM elements in Fig. 2(a). The probability of success for discriminating the states is given by

$$P_s = \tfrac{1}{2} + \tfrac{1}{4}\sin(4\theta). \tag{3}$$

The experimental result of the state discrimination is illustrated in Fig. 4(a). For $\theta = 0^\circ$, P_s is the same as the probability of success for determining the second measurement result. However, for other values of θ, a different phenomenon arises compared with determining the second measurement result. After P_s increases to a maximum value of $3/4$ at $\theta = \pi/8$, it decreases back to $1/2$ at $\theta = \pi/4$. This is because the second measurement becomes closer to a projection measurement as θ tends to $\pi/4$, which eliminates the correlation between the first measurement and the final state. Furthermore, the second measurement makes the ρ_{1+} and ρ_{1-} become less distinguishable as θ approaches $\pi/4$. As before, using Bayes's theorem, we present a comparison of $P(\rho_{1+})$ and $P(\rho_{1+}|M_{\text{out}}=+)$ in Fig. 4(b).

V. RETRODICTION OF THE TRAJECTORY

Finally, we determine the results of both measurements, so the four output states should be discriminated (see Appendix B for the specific form of the states). We use a strong method, the square-root measurement (see Appendix C for details), to discriminate the output states [10,39]. The POVM elements for square-root measurement are given by $\Pi_{jk} = \frac{1}{4}|\widetilde{\Psi}^{jk}\rangle\langle\widetilde{\Psi}^{jk}|$, where $j,k = \pm$, and the states $|\widetilde{\Psi}^{++}\rangle = (\cos\theta - \sin\theta)|+\rangle - (\sin\theta + \cos\theta)|-\rangle$, $|\widetilde{\Psi}^{+-}\rangle = (\cos\theta + \sin\theta)|+\rangle + (\sin\theta - \cos\theta)|-\rangle$, $|\widetilde{\Psi}^{-+}\rangle = (\cos\theta - \sin\theta)|+\rangle + (\sin\theta + \cos\theta)|-\rangle$, $|\widetilde{\Psi}^{--}\rangle = (\cos\theta + \sin\theta)|+\rangle - (\sin\theta - \cos\theta)|-\rangle$. The measurement setup for realizing the POVM elements is shown in Fig. 2(c). The probability of success for identifying the states is expressed as

$$P_s = \tfrac{1}{4}[1 + \sin(2\theta) + \sin^2(2\theta) - \sin^3(2\theta)]. \tag{4}$$

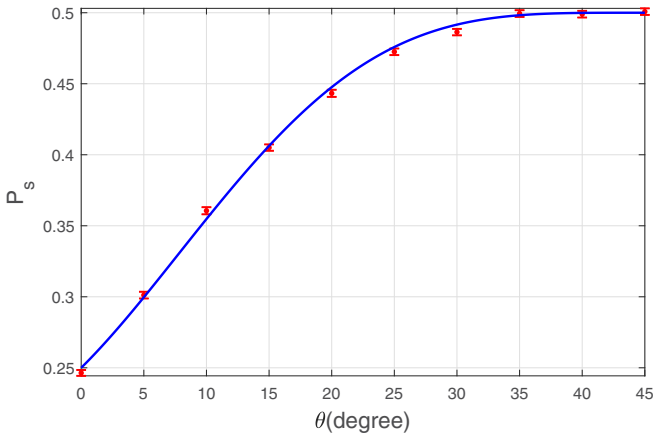

FIG. 5. Experimental results for the relationship between different POVMs and retrodiction of both the first and second measurements. The blue line is the theoretical expectations; the red dots are values from experimental data.

From the experimental results for state discrimination (Fig. 5), at $\theta = 0^\circ$, the four output states become $|+\rangle$. There is therefore no correlation between measurement results and the final states, and we cannot extract trajectory information of the photon by discriminating the final states. At $\theta = 45^\circ$, the first and second measurements both become projection measurements, so the probability of success is maximum; moreover, from Figs. 3(a) and 4(a), we see that the trajectory of the photon passing through the second interferometer is determined with certainty, but all trajectory information from passing through the first interferometer is lost.

VI. CONCLUSIONS

To summarize, in a set with double interferometers, we experimentally retrodicted the trajectories of single photons by measuring the final state of the photon. We obtained the probability of success for determining the partial trajectories and the entire trajectories by discriminating the final states of the photon. Moreover, we also observed the effect of different measurements on the extraction of trajectory information. If the second measurement is a projection measurement, it erases the trajectory information of the photon passing through the first interferometer. If both measurements are projection measurements, we obtain maximum trajectory information of the photon passing through the double interferometers. Because the photon carries information about the history of measurements on it and this information can be extracted by measuring the final state of the photon, this could be useful in quantum communication schemes. Indeed, our experiment highlights the application of retrodiction theory to the study of a photon's past, and provides potential application in the field of quantum communications.

ACKNOWLEDGMENTS

This work is supported by the National Natural Science Foundation of China (Grants No. 11574291 and No. 11774334), China Postdoctoral Science Foundation (Grant No. 2016M602012).

APPENDIX A: DETAILS FOR THE SINGLE-PHOTON SOURCE MODULE OF THE EXPERIMENTAL SETUP

In the single-photon source module, a 80-mW cw laser with a 404-nm wavelength (linewidth=5 MHz) pumps a type-II beamlike phase-matching beta-barium-borate (BBO, $6.0\times6.0\times2.0$ mm^3, $\theta = 40.98^\circ$) crystal to produce a pair of photons with wavelength $\lambda = 808$ nm. After being redirected by mirrors and passed through the interference filters ($\triangle\lambda = 3$ nm, $\lambda = 808$ nm), the photon pairs generated in spontaneous parametric down-conversion are coupled into single-mode fibers separately. One photon is detected by a single-photon detector acting as a trigger. The total coincidence counts are approximately 4×10^3 per second. According to measurement method for the $g^2(\tau)$ of heralded single-photon sources [40–42], we obtain the time-averaged conditional coherence functions $\overline{g}_c^2(0)$ as 0.0025 ± 0.0051.

APPENDIX B: SPECIFIC FORM OF STATE

Different measurement results correspond to the different final states of the photon. After the second measurement, the final output states of the photon for the different measurement results are given by

$$
\begin{aligned}
|\Psi_{\text{out}}^{++}\rangle &= \frac{1}{[1-\sin(2\theta)\cos(2\theta)]^{1/2}}[\cos\theta(\cos\theta-\sin\theta)|+\rangle \\
&\quad -\sin\theta(\sin\theta+\cos\theta)|-\rangle], \\
|\Psi_{\text{out}}^{+-}\rangle &= \frac{1}{[1+\sin(2\theta)\cos(2\theta)]^{1/2}}[\cos\theta(\cos\theta+\sin\theta)|+\rangle \\
&\quad +\sin\theta(\sin\theta-\cos\theta)|-\rangle], \\
|\Psi_{\text{out}}^{-+}\rangle &= \frac{1}{[1-\sin(2\theta)\cos(2\theta)]^{1/2}}[\cos\theta(\cos\theta-\sin\theta)|+\rangle \\
&\quad +\sin\theta(\sin\theta+\cos\theta)|-\rangle], \\
|\Psi_{\text{out}}^{--}\rangle &= \frac{1}{[1+\sin(2\theta)\cos(2\theta)]^{1/2}}[\cos\theta(\cos\theta+\sin\theta)|+\rangle \\
&\quad -\sin\theta(\sin\theta-\cos\theta)|-\rangle].
\end{aligned} \tag{B1}
$$

The joint probabilities for the two measurements are expressed as $P(+,+) = \text{Tr}(A_+ H A_+|+\rangle\langle+|A_+^\dagger H A_+^\dagger) = [1 - \sin(2\theta)\cos(2\theta)]/4$. Similarly, we find $P(-,+) = P(+,+)$ and $P(+,-) = P(-,-) = [1 + \sin(2\theta)\cos(2\theta)]/4$.

If the first measurement result is ignored, the density matrix corresponding to the second measurement result $+$ is ρ_{2+}, which appears with probability $P(\rho_{2+}) = P(+,+) + P(-,+) = [1 - \sin(2\theta)\cos(2\theta)]/2$; the density matrix corresponding to the second measurement result $-$ is ρ_{2-}, which appears with a probability of $P(\rho_{2-}) = P(+,-) + P(-,-) = [1 + \sin(2\theta)\cos(2\theta)]/2$. ρ_{2+} and ρ_{2-} are expressed as

$$
\begin{aligned}
\rho_{2+} &= [P(+,+)|\Psi_{\text{out}}^{++}\rangle\langle\Psi_{\text{out}}^{++}| \\
&\quad + P(-,+)|\Psi_{\text{out}}^{-+}\rangle\langle\Psi_{\text{out}}^{-+}|]/P(\rho_{2+}), \\
\rho_{2-} &= [P(+,-)|\Psi_{\text{out}}^{+-}\rangle\langle\Psi_{\text{out}}^{+-}| \\
&\quad + P(-,-)|\Psi_{\text{out}}^{--}\rangle\langle\Psi_{\text{out}}^{--}|]/P(\rho_{2-}).
\end{aligned} \tag{B2}
$$

If the second measurement result is ignored, the density matrices corresponding to the first measurement results $+$ and

− are denoted as ρ_{1+} and ρ_{1-}, which are expressed as

$$\begin{aligned}\rho_{1+} &= [P(+,+)|\Psi_{\text{out}}^{++}\rangle\langle\Psi_{\text{out}}^{++}| \\ &\quad + P(+,-)|\Psi_{\text{out}}^{+-}\rangle\langle\Psi_{\text{out}}^{+-}|]/P(\rho_{1+}), \\ \rho_{1-} &= [P(-,+)|\Psi_{\text{out}}^{-+}\rangle\langle\Psi_{\text{out}}^{-+}| \\ &\quad + P(-,-)|\Psi_{\text{out}}^{--}\rangle\langle\Psi_{\text{out}}^{--}|]/P(\rho_{1-}). \end{aligned} \tag{B3}$$

These two density matrices appear with a probability of $P(\rho_{1+}) = P(\rho_{1-}) = 1/2$.

APPENDIX C: SQUARE-ROOT MEASUREMENT

The square-root measurement is a pretty good state discrimination measurement [39]. For a given set of states $\{|\Psi_{\text{out}}^{jk}\rangle|j,k = \pm\}$ we can construct an associated measurement, the square-root measurement, to discriminate them. The POVM elements for the square-root measurement are given by

$$\Pi_{jk} = P(j,k)\rho^{-1/2}|\Psi_{\text{out}}^{jk}\rangle\langle\Psi_{\text{out}}^{jk}|\rho^{-1/2}, \tag{C1}$$

where $P(j,k)$ is a probability that the state $|\Psi_{\text{out}}^{jk}\rangle$ appeared, and $\rho = P(+,+)|\Psi_{\text{out}}^{++}\rangle\langle\Psi_{\text{out}}^{++}| + P(+,-)|\Psi_{\text{out}}^{+-}\rangle\langle\Psi_{\text{out}}^{+-}| + P(-,+)|\Psi_{\text{out}}^{-+}\rangle\langle\Psi_{\text{out}}^{-+}| + P(-,-)|\Psi_{\text{out}}^{--}\rangle\langle\Psi_{\text{out}}^{--}|$. According to Eq. (B1) and the expression of $P(j,k)$, we obtain $\rho = \cos^2\theta|+\rangle\langle+| + \sin^2\theta|-\rangle\langle-|$ and $\rho^{-1/2} = (1/\cos\theta)|+\rangle\langle+| + (1/\sin\theta)|-\rangle\langle-|$. Hence $\Pi_{jk} = \frac{1}{4}|\widetilde{\Psi}^{jk}\rangle\langle\widetilde{\Psi}^{jk}|$ with the states

$$\begin{aligned}|\widetilde{\Psi}^{++}\rangle &= (\cos\theta - \sin\theta)|+\rangle - (\sin\theta + \cos\theta)|-\rangle, \\ |\widetilde{\Psi}^{+-}\rangle &= (\cos\theta + \sin\theta)|+\rangle + (\sin\theta - \cos\theta)|-\rangle, \\ |\widetilde{\Psi}^{-+}\rangle &= (\cos\theta - \sin\theta)|+\rangle + (\sin\theta + \cos\theta)|-\rangle, \\ |\widetilde{\Psi}^{--}\rangle &= (\cos\theta + \sin\theta)|+\rangle - (\sin\theta - \cos\theta)|-\rangle. \end{aligned} \tag{C2}$$

[1] S. M. Barnett, D. T. Pegg, and J. Jeffers, J. Mod. Opt. **47**, 1779 (2000).
[2] S. M. Barnett, D. T. Pegg, J. Jeffers, O. Jedrkiewicz, and R. Loudon, Phys. Rev. A **62**, 022313 (2000).
[3] O. Jedrkiewicz, R. Loudon, and J. Jeffers, Phys. Rev. A **70**, 033805 (2004).
[4] A. H. Werner, T. Franz, and R. F. Werner, Phys. Rev. Lett. **103**, 220504 (2009).
[5] D. T. Pegg and S. M. Barnett, J. Opt. B: Quantum Semiclass. Opt. **1**, 442 (1999).
[6] A. Chefles and M. Sasaki, Phys. Rev. A **67**, 032112 (2003).
[7] S. M. Barnett, *Quantum Information and Coherence* (Springer, Heidelberg, 2014).
[8] D. T. Pegg, S. M. Barnett, and J. Jeffers, Phys. Rev. A **66**, 022106 (2002).
[9] S. M. Barnett, D. T. Pegg, J. Jeffers, and O. Jedrkiewicz, Phys. Rev. Lett. **86**, 2455 (2001).
[10] M. Hillery and D. Koch, Phys. Rev. A **94**, 032118 (2016).
[11] O. Jedrkiewicz, R. Loudon, and J. Jeffers, Eur. Phys. J. D **39**, 129 (2006).
[12] M. Sonnleitner, J. Jeffers, and S. M. Barnett, Optica **2**, 950 (2015).
[13] F. C. Speirits, M. Sonnleitner, and S. M. Barnett, J. Opt. **19**, 044001 (2017).
[14] D. Tan, S. J. Weber, I. Siddiqi, K. Mølmer, and K. W. Murch, Phys. Rev. Lett. **114**, 090403 (2015).
[15] P. Ghose, A. S. Majumdar, S. Guha, and J. Sau, Phys. Lett. A **290**, 205 (2001).
[16] V. Jacques, E. Wu, F. Grosshans, F. Treussart, P. Grangier, A. Aspect, and J.-F. Roch, Science **315**, 966 (2007).
[17] V. Jacques, E. Wu, F. Grosshans, F. Treussart, P. Grangier, A. Aspect, and J.-F. Roch, Phys. Rev. Lett. **100**, 220402 (2008).
[18] A. Peruzzo, P. Shadbolt, N. Brunner, S. Popescu, and J. L. O'Brien, Science **338**, 634 (2012).
[19] F. Kaiser, T. Coudreau, P. Milman, D. B. Ostrowsky, and S. Tanzilli, Science **338**, 637 (2012).
[20] L. Vaidman, Phys. Rev. A **87**, 052104 (2013).
[21] A. Danan, D. Farfurnik, S. Bar-Ad, and L. Vaidman, Phys. Rev. Lett. **111**, 240402 (2013).
[22] Z.-Q. Zhou, X. Liu, Y. Kedem, J.-M. Cui, Z.-F. Li, Y.-L. Hua, C.-F. Li, and G.-C. Guo, Phys. Rev. A **95**, 042121 (2017).
[23] D. Paneru and E. Cohen, International Journal of Quantum Information **15**, 1740019 (2017).
[24] Y. Aharonov and L. Vaidman, Lect. Notes Phys. **734**, 399 (2008).
[25] Y. Aharonov, P. G. Bergmann, and J. L. Lebowitz, Phys. Rev. **134**, B1410 (1964).
[26] Y. Aharonov and L. Vaidman, Phys. Rev. A **41**, 11 (1990).
[27] V. Potoček and G. Ferenczi, Phys. Rev. A **92**, 023829 (2015).
[28] B.-G. Englert, K. Horia, J. Dai, Y. L. Len, and H. K. Ng, Phys. Rev. A **96**, 022126 (2017).
[29] B.-G. Englert, Phys. Rev. Lett. **77**, 2154 (1996).
[30] S. Dürr, T. Nonn, and G. Rempe, Phys. Rev. Lett. **81**, 5705 (1998).
[31] M. N. Bera, T. Qureshi, M. A. Siddiqui, and A. K. Pati, Phys. Rev. A **92**, 012118 (2015).
[32] E. Bagan, J. A. Bergou, S. S. Cottrell, and M. Hillery, Phys. Rev. Lett. **116**, 160406 (2016).
[33] Y. Yuan, Z. Hou, Y.-Y. Zhao, H.-S. Zhong, G.-Y. Xiang, C.-F. Li, and G.-C. Guo, Opt. Express **26**, 4470 (2018).
[34] Z. Bian, J. Li, H. Qin, X. Zhan, R. Zhang, B. C. Sanders, and P. Xue, Phys. Rev. Lett. **114**, 203602 (2015).
[35] Y. Y. Zhao, N. K. Yu, P. Kurzynski, G. Y. Xiang, C. F. Li, and G. C. Guo, Phys. Rev. A **91**, 042101 (2015).
[36] Z. Hou, J.-F. Tang, J. Shang, H. Zhu, J. Li, Y. Yuan, K.-D. Wu, G.-Y. Xiang, C.-F. Li, and G.-C. Guo, Nat. Commun. **9**, 1414 (2018).
[37] F. Piacentini, A. Avella, E. Rebufello, R. Lussana, F. Villa, A. Tosi, M. Gramegna, G. Brida, E. Cohen, L. Vaidman, I. P. Degiovanni, and M. Genovese, Nature Phys. **13**, 1191 (2017).
[38] C. W. Helstrom, *Quantum Detection and Estimation Theory* (Academic, New York, 1976).
[39] S. M. Barnett and S. Croke, Adv. Opt. Photonics **1**, 238 (2009).
[40] E. Bocquillon, C. Couteau, M. Razavi, R. Laflamme, and G. Weihs, Phys. Rev. A **79**, 035801 (2009).
[41] M. Razavi, I. Söllner, E. Bocquillon, C. Couteau, R. Laflamme, and G. Weihs, J. Phys. B **42**, 114013 (2009).
[42] D. Höckel, L. Koch, and O. Benson, Phys. Rev. A **83**, 013802 (2011).